



Assessment of the Aging Process of Finished Product–Modified Asphalt Binder and Its Aging Mechanism

Dongdong Yuan¹; Wei Jiang²; Jingjing Xiao³; Zheng Tong⁴; Meng Jia⁵; Jinshan Shan⁶; and Aboudou Wassiou Ogbon⁷

Abstract: Styrene-butadiene-styrene-modified asphalt binder (SBSMA), crumb rubber-modified asphalt binder (CRMA), and high-viscosity-modified asphalt binder (HVMA) have been widely used in porous asphalt concrete. However, the aging of the modified asphalt binder significantly affects the performance of the porous asphalt concrete. The main aim of this research is to quantitatively assess the aging degree of finished product-modified asphalt binders of SBSMA, CRMA, and HVMA at high, medium, and low temperatures, and to explore the aging mechanism at the microscopic level. This study used rolling thin-film oven and pressurized aging vessel to simulate the aging of asphalt binders. Dynamic shear rheometer, bending beam rheometer, Fourier transform infrared spectrometry, thin-layer chromatography with flame ionization detection, and scanning electron microscopy were employed to investigate how aging affects the rheological and microscopic properties of finished product-modified asphalt binder. The results showed that at high temperatures, short-term aging significantly impacted HVMA [change rate of the rutting factor (CRRF) = 18.9%], while long-term aging had an enormous influence on CRMA (CRRF = 179.5%). Short-term aging had the greatest effect on the fatigue property at medium temperature of CRMA [change rate of N_f (CRN_f) = 59.9%], followed by SBSMA (CRN_f = 46.1%) and HVMA (CRN_f = 26.2%). However, the effect of long-term aging on the fatigue properties of HVMA (CRN_f = 99.2%) is the largest, followed by that of CRMA (CRN_f = 95.8%) and SBSMA (CRN_f = 56.6%). At low temperature, compared with CRMA and HVMA, aging had the greatest influence on the low-temperature rheological properties of SBSMA. In addition, the three finished product-modified asphalt binders exhibited similar changes in microscopic level after aging. DOI: [10.1061/\(ASCE\)MT.1943-5533.0004330](https://doi.org/10.1061/(ASCE)MT.1943-5533.0004330). © 2022 American Society of Civil Engineers.

Author keywords: Finished product-modified asphalt binder; Asphalt aging; Aging degree; Rheological properties; Microscopic level.

Introduction

Porous asphalt concrete is a kind of pavement material with a porosity of 16% to 25% (Jiang et al. 2018; Cai et al. 2019). Compared with traditional dense pavement materials that have full area contact between aggregates, aggregates in porous asphalt concrete have point contact with each other (Jiang et al. 2018; Zhang et al. 2020; Han et al. 2021). This leads to the reduction of bonding

contact area between porous asphalt concrete aggregate (Jiang et al. 2020). Therefore, modified asphalt binders are usually used in porous asphalt concrete to ensure its strength, stability, and durability (Alvarez et al. 2010; Cong et al. 2010). Generally, elastomer-modified asphalt binders with polymer-rich phases such as styrene-butadiene-styrene-modified asphalt (SBSMA), crumb rubber-modified asphalt (CRMA), and high-viscosity-modified asphalt (HVMA) have widely been used in porous asphalt concrete due to their excellent road performance (Leng et al. 2018; Wei et al. 2019; Hu et al. 2020b). However, due to different application environments, there are differences in the selection of modified asphalt binders in different regions. SBSMA and CRMA are always used in the United States and Europe (Frigo et al. 2015). In China, Japan, and Singapore, HVMA is commonly used (Moriyoshi et al. 2013). However, modified asphalt binder is prone to aging during the construction and service stages of asphalt pavements (Hossain et al. 2018; Cai et al. 2020). The aging conditions of the modified asphalt binder can be divided into two parts: short- and long-term aging. Short-term aging refers to the aging process of an asphalt binder during construction, whereas long-term aging occurs during the pavement service period. Currently, the methods used for simulating the short- and long-term aging processes of asphalt binders are rolling thin-film oven test (RTFOT) and pressurized aging vessel (PAV), respectively (Bi et al. 2020).

¹Ph.D. Student, School of Highway, Chang'an Univ., Xi'an, Shaanxi 710064, PR China. Email: ddy@chd.edu.cn

²Professor, School of Highway, Chang'an Univ., Xi'an, Shaanxi 710064, PR China; Professor, Key Laboratory for Special Area Highway Engineering of Ministry of Education, Chang'an Univ., Xi'an, Shaanxi 710064, PR China (corresponding author). Email: jiangwei@chd.edu.cn

³Assistant Professor, School of Civil Engineering, Chang'an Univ., Xi'an, Shaanxi 710061, PR China. Email: xiaojj029@sina.com

⁴Ph.D. Student, School of Highway, Chang'an Univ., Xi'an, Shaanxi 710064, PR China. Email: zheng.tong@hds.utc.fr

⁵Ph.D. Student, School of Highway, Chang'an Univ., Xi'an, Shaanxi 710064, PR China. Email: mengjia@chd.edu.cn

⁶Ph.D. Student, School of Highway, Chang'an Univ., Xi'an, Shaanxi 710064, PR China. Email: jhshan@chd.edu.cn

⁷Ph.D. Student, School of Highway, Chang'an Univ., Xi'an, Shaanxi 710064, PR China. Email: atchaniogbon@yahoo.com

Note. This manuscript was submitted on May 18, 2021; approved on December 9, 2021; published online on May 24, 2022. Discussion period open until October 24, 2022; separate discussions must be submitted for individual papers. This paper is part of the *Journal of Materials in Civil Engineering*, © ASCE, ISSN 0899-1561.

Some researchers and engineers have explored the influence of aging on the properties of modified asphalt. Studies have indicated changes in the physical properties of modified asphalt binder before and after aging, such as penetration, softening point, and ductility

(Wu et al. 2006). In fact, these physical properties cannot effectively describe the viscoelastic characteristics of modified asphalt binders (Yan et al. 2019a). Therefore, the rheological properties measured using a dynamic shear rheometer (DSR) and bending beam rheometer (BBR) are commonly used to evaluate the aging degree of modified asphalt binders. Zhu (2015) used a DSR to compare the effects of aging on the rheological properties of neat asphalt, 3.0% SBSMA, and 7.5% SBSMA. The results showed that the rheological properties of 7.5% SBSMA were the least susceptible to aging, followed by 3.0% SBSMA and neat asphalt. Fethiza Ali et al. (2020) investigated changes in the complex modulus of CRMA after aging. The results showed that CRMA became hard and brittle after aging, and the complex modulus increased. Ma et al. (2017) and Ding et al. (2019) demonstrated that the properties of CRMA are similar to those of SBSMA after aging. Hu et al. (2020c) studied the changes in the rheological properties of neat asphalt, HVMA, and SBSMA during the aging process. The results indicated that the rotational viscosity and strain recovery of HVMA initially decreased and then increased with aging. The aging resistance of HVMA was better than that of neat asphalt and SBSMA. However, there are relatively few comparisons of the rheological properties of SBSMA, CRMA, and HVMA after aging. In addition, with the development of science and technology, researchers have focused on the microstructure of the modified asphalt binder after aging. A series of modern tests have been applied, such as Fourier transform infrared spectrometry (FT-IR), thin-layer chromatography with flame ionization detection (TLC-FID), and scanning electron microscopy (SEM) (Liu et al. 2018; Wang et al. 2018; Ye et al. 2019). After aging, asphalt will undergo a series of chemical reactions, resulting in short-chain compounds undergoing additive, polymerization, oxidative dehydrogenation, and other reactions. The complex structures of cyclic compounds and carbonyl, sulfoxide, and other polar functional groups are generated. Increasing the molecular weight of asphalt by increasing the fraction of light components such as aromatic to heavy components such as asphaltene, causes asphalt hardening, fatigue cracking, and other diseases.

Based on the preceding analysis, rheological properties and microstructure tests have significant advantages for research on modified asphalt aging. Many researchers have conducted systematic studies on the aging behavior of modified asphalt binders prepared in small batches in the laboratory and achieved meaningful results. However, few researchers have focused on the aging behavior of finished product-modified asphalt binders. In fact, research on the aging behavior of finished product-modified asphalt binders has practical significance in engineering. Therefore, the finished product-modified asphalt binders of SBSMA, CRMA, and HVMA were selected as the research objects of this study.

The main aim of this research is to quantitatively assess the aging degree of finished product-modified asphalt binders SBSMA, CRMA, and HVMA at high, medium, and low temperatures, and to explore the aging mechanism at a microscopic level. First, SBSMA, CRMA, HVMA, and reference neat asphalt were aged using RTFOT and PAV. Second, a series of rheological property tests, such as the temperature sweep test, linear amplitude sweep (LAS) test, and BBR test, were used to study the effects of aging on the rheological properties of the finished product-modified asphalt binders. Subsequently, the FT-IR, TLC-FID, and SEM tests were used to investigate microscopic properties in the finished product-modified asphalt binders during the aging process. Finally, a series of aging degree indexes, such as the change rate of the rutting factor (CRRF), change rate of N_f (CRN_f), and change rate of ΔT_c ($CR\Delta T_c$), were proposed to compare the aging resistance of the finished product-modified asphalt binders.

Table 1. Properties of neat asphalt, SBSMA, CRMA, and HVMA

Property	Neat asphalt	SBSMA	CRMA	HVMA
Penetration at 25°C (0.1 mm)	97.1	64.0	51.1	49.3
Softening point (°C)	47.4	94.2	63.2	94.2
Ductility at 5°C (cm)	—	45.7	13.3	48.6
Dynamic viscosity at 60°C (Pa·s)	140.3	14,169.2	3,177.7	99,635.4

Experimental Materials and Methodologies

Materials

In this study, three types of modified asphalt binders were analyzed: SBSMA, CRMA, and HVMA. Additionally, the neat asphalt SK-90 was used as a reference. The neat asphalt was produced by SK Holdings (Seoul). SBSMA, CRMA, and HVMA are finished product-modified asphalt binders, which were supplied by local manufacturers in China. The contents of SBS, crumb rubber, and high-viscosity modifier in SBSMA, CRMA, and HVMA were 4.5% (Sumit et al. 2022), 15% (Israel et al. 2020), and 12% (Jiang et al. 2021), respectively. For SBSMA, the SBS was linear, and the ratio of styrene to butadiene was 30:70. The temperature of mixing was 170°C, the shear rate was 2,900 rpm, and the duration of mixing was 120 min. For CRMA, the crumb rubber was obtained by treating radial tire at ambient temperature, which size is 60 mesh. The temperature of mixing was 185°C, the shear rate was 2,900 rpm, and the duration of mixing was 120 min. For HVMA, the viscosity enhancer was synthetic based. The temperature of mixing was 180°C, the shear rate was 4,500 rpm, and the duration of mixing was 30 min. Table 1 lists the main physical properties of the neat asphalt, SBSMA, CRMA, and HVMA.

Test Methodologies

This study was conducted according to the procedures shown in Fig. 1. First, a short-term aging and long-term aging experiment was carried out in the laboratory on the three asphalt binders and the neat asphalt. Second, the rheological properties of different modified asphalt binders at high, medium, and low temperatures were studied as well as the changes in the microscopic level of the asphalt binders after aging were investigated. Finally, the aging characteristics of the different asphalt binders were compared.

Laboratory Aging

The short-term aging and long-term aging of the four asphalt samples were simulated using the standard RTFOT (163°C, 85 min, 15 rpm, 4,000 mL/min) and PAV tests (100°C, 20 h, 2.1 MPa) according to ASTM D2872-19 (ASTM 2019b) and ASTM D6521-19a (ASTM 2019a), respectively.

Dynamic Shear Rheometer Test

A TA HR-1 DSR (TA Instruments, New Castle, Delaware) was used to test the high-temperature properties and fatigue properties (at medium temperature). One sample per replicate was used in the temperature sweep test. However, repeated tests were performed on several samples, and the deviations of the repeated tests were small because of the high precision of the DSR. Thus, in this study, the temperature sweep tests were not replicated. The linear amplitude sweep test was replicated three times and the average of those three tests was used to determine the results.

Temperature sweep tests were performed to study the high-temperature properties of the asphalt binders. The temperature

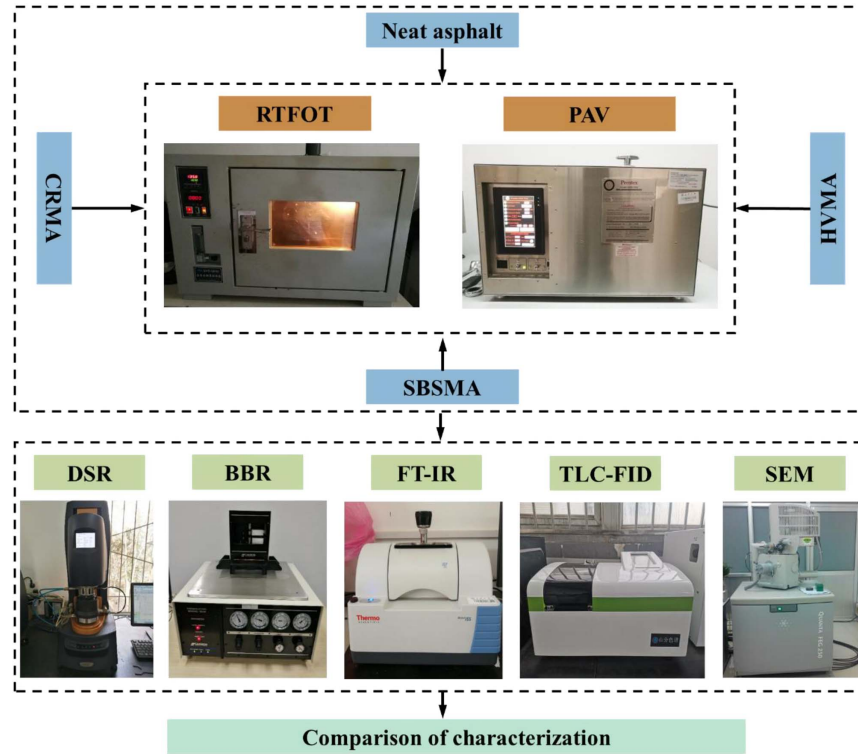


Fig. 1. Procedure of this study.

sweep tests were conducted at 30°C, 40°C, 50°C, 60°C, 70°C, and 80°C at an angular frequency of 10 rad/s.

LAS tests were used to study the asphalt binder fatigue properties at medium temperature. Two steps were involved: a frequency sweep test (the strain was 0.1% and the frequency ranged from 0.1 to 30 Hz) and an amplitude sweep test (the frequency was 10 Hz and the strain was 0.1%–30%) at 25°C.

Bending Beam Rheometer Test

BBR tests (ASTM 2016) were used to evaluate the low-temperature properties of the aged binders. The tests were implemented at -12°C, -18°C, and -24°C. The tests were conducted using a TE-BBR (Cannon, Tokyo). Three replicate samples were used in the BBR test, which met the requirements of the specifications issued by ASTM/AASHTO [ASTM D6648-08(2016)] (ASTM 2016); AASHTO TP 125 (AASHTO 2016a)].

Fourier Transform Infrared Spectrometry Test

FT-IR is regarded as a promising method to evaluate the aging effect on a binder because of its accuracy and sensitivity (Yan et al. 2018; Fini et al. 2011). Infrared spectra were obtained using a Thermo Fisher Scientific Nicolet iS5 FT-IR spectrometer (Thermo Fisher Scientific, Shanghai, China). Three replicate samples were used in the FT-IR test, and the average of three replicate tests was used as the final result.

Thin-Layer Chromatography with Flame Ionization Detection Test

The TLC-FID test is a rapid, convenient, efficient, and accurate method for the analysis of asphalt components (asphaltenes, resins, saturates, aromatics). The test was executed according to ASTM D4124-18 (ASTM 2018). The instrument used in TLC-FID analysis was a SF-16A by Zibo Shanfen Analytical Instrument Co., Ltd (Shanfen Analttical Instrument, Zibo, China).

Scanning Electron Microscopy Test

The asphalt binder samples were examined by FEI Quanta FEG250 scanning electron microscope (Hillsboro, Hillsboro, Oregon). First, the asphalt binders were heated to a molten state. Second, a thin layer of asphalt binders was scraped on the test bench. In addition, because the asphalt binders are not conductive, it is necessary to spray gold on the thin-layer sample.

Results and Discussion

High-Temperature Properties Analysis

Complex Modulus and Phase Angle

The complex modulus (G^*) can be used to measure the high-temperature deformation resistance of the asphalt binder (Gao et al. 2019). The phase angle (δ) can indicate the viscosity and elasticity ratio of bitumen to some extent (Dai et al. 2021). Fig. 2 shows the G^* and δ values of the four asphalt samples under different aging conditions. It can be seen that the free volume of the asphalt binder increases while the asphalt binder intermolecular force decreases. There were few changes in the complex moduli of the four asphalt samples after RTFOT. After PAV, there was an increase in all complex moduli. Except for the unaged SBSMA, phase angles of the other bitumen increased as temperature increased. In unaged SBSMA, the phase angle exhibits a descending trend with increasing temperature. This tendency trend is attributed to the dominance of the polymer phase at high temperatures. At high temperatures, the viscosity of neat asphalt is low enough for the polymer network to exert more influence on the mechanical properties of the modified binder, and thus it exhibits a lower phase angle (Yan et al. 2019b). Some studies showed the phase angle of SBSMA will decline at lower frequency (Airey 2003; Asgharzadeh et al. 2013; Yusoff et al. 2013) (which correspond to high temperature

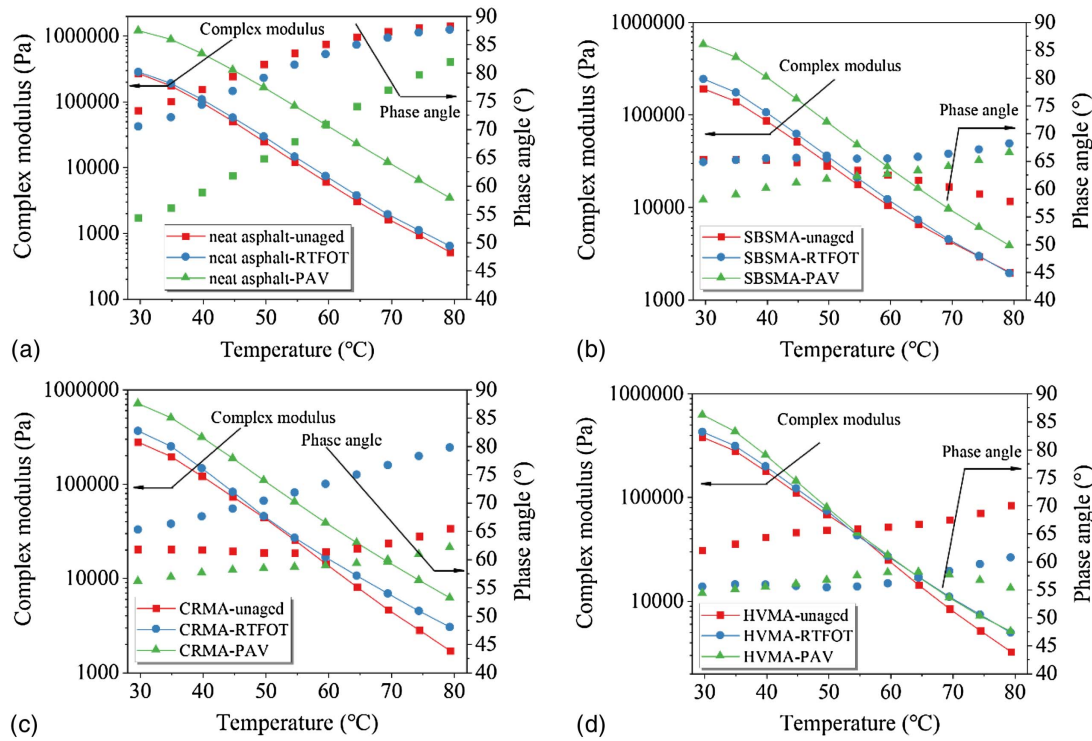


Fig. 2. Changes in the complex modulus and phase angle with temperature: (a) neat asphalt; (b) SBSMA; (c) CRMA; and (d) HVMA.

according to the time–temperature equivalence rule). Phase angle decreased with aging for neat asphalt, suggesting that hardening was occurring due to aging. However, phase angles did not change regularly after aging for SBSMA, CRMA, and HVMA. This was probably due to the swelling or degradation of SBS, crumb rubber, and high-viscosity modifier after RTFOT and PAV aging, which changes the elastic and viscous ratio of the modified asphalt (Naderi et al. 2014; Tang et al. 2019).

Fig. 3 shows the complex modulus change rate of different asphalts before and after aging. The rate of change of the complex modulus can be calculated using Eq. (1). A higher change rate in the complex modulus indicates aging has a greater influence on the asphalt binder's complex modulus (Wang et al. 2020; Lyu et al. 2021). In Fig. 3, PAV aging had a greater effect on the complex modulus than RTFOT aging for all four asphalt samples. When

compared with modified asphalt binders, PAV aging had the greatest effect on neat asphalt. For SBSMA, CRMA, and HVMA, PAV aging had the greatest effect on SBSMA when the temperature was less than 55°C. When the temperature was higher than 55°C, PAV aging had the greatest effect on CRMA. This may be caused by the activity of the SBS modifier increasing when the temperature exceeded 55°C. In comparison with SBSMA and HVMA, RTFOT aging has the greatest effect on CRMA

Change rate of complex modulus

$$= \frac{\text{Aged complex modulus} - \text{Unaged complex modulus}}{\text{Unaged complex modulus}} \times 100 \quad (1)$$

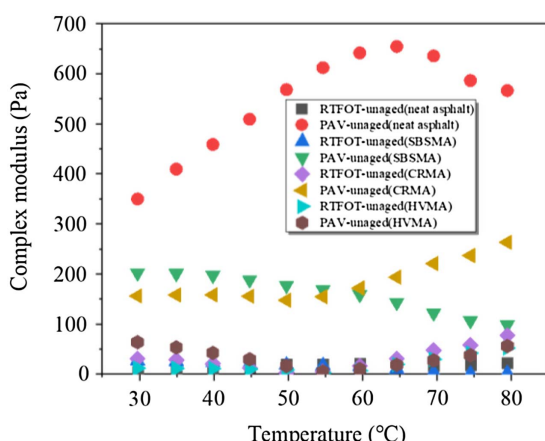


Fig. 3. Change rate of the complex modulus of different asphalts after aging.

Rutting Factor and Its Change Rate

The rutting factor ($G^*/\sin \delta$) is an index that expresses the rutting performance of asphalt at high temperature (Zhang et al. 2018). Fig. 4 illustrates the rutting factors for neat asphalt, SBSMA, CRMA, and HVMA under different conditions. As seen in Fig. 4, the rutting factors of neat asphalt, SBSMA, CRMA, and HVMA increase with aging. This indicates that aging can enhance the high-temperature stability of asphalt binder. For neat asphalt, this may have been due to thermal oxidation. For SBSMA, CRMA, and HVMA, it may have been caused by the thermal oxidation of neat asphalt and the swelling and decomposition of the polymer modifier (Li et al. 2020a).

The CRRF can be used to determine the aging degree of the asphalt binder at high temperatures (Zhang and Jia 2019). The formula for calculating the CRRF is shown in Eq. (2). Higher CRRF normally indicates more serious aging degree of the asphalt binder (Zhang et al. 2018). Previous studies have generated promising results to adopt CRRF at 60°C. Fig. 5 presents the CRRF of neat asphalt, SBSMA, CRMA, and HVMA. It can be seen that the

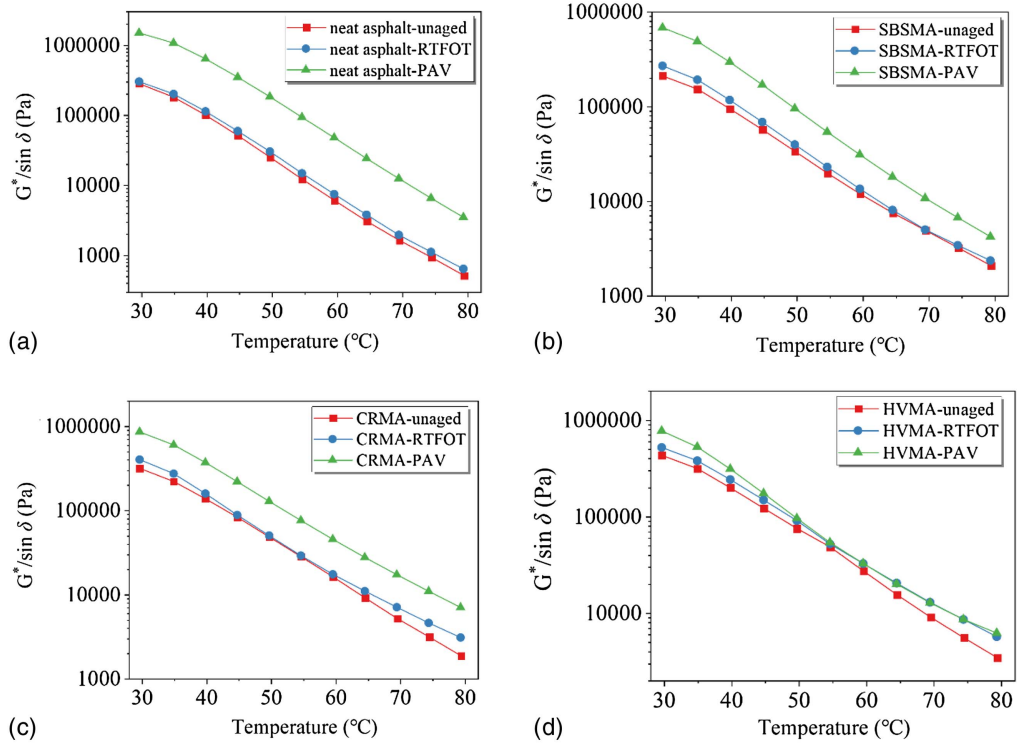


Fig. 4. Changes in rutting factor with temperature: (a) neat asphalt; (b) SBSMA; (c) CRMA; and (d) HVMA.

CRRF of the four samples after RTFOT is as follows: neat asphalt (22.6%) > HVMA (18.9%) > SBSMA (12.6%) > CRMA (7.1%). The ranking of CRRF after PAV is neat asphalt (682.8%) > CRMA (179.5%) > SBSMA (159.0%) > HVMA (19.3%). As compared to the modified asphalts, neat asphalt showed the greatest CRRF, indicating that aging affected it the most at high temperatures.

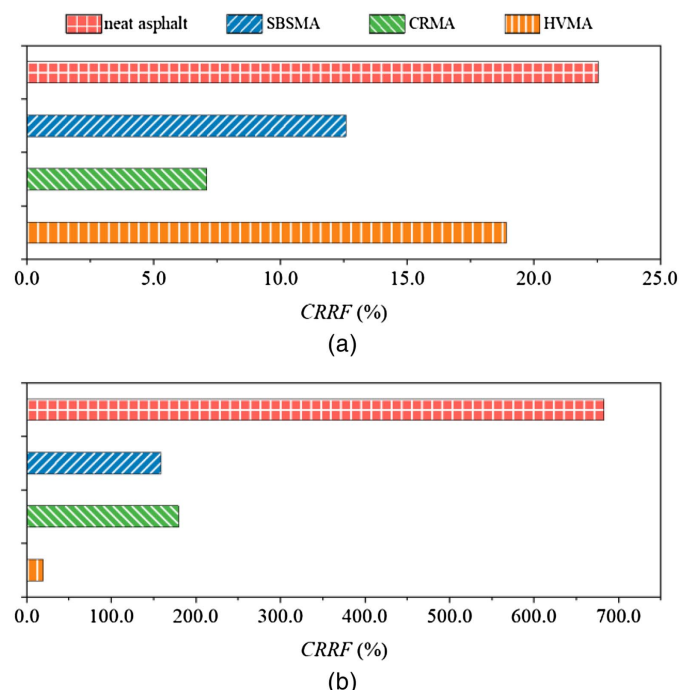


Fig. 5. CRRF of neat asphalt, SBSMA, CRMA and HVMA: (a) RTFOT; and (b) PAV.

The effect of aging on the modified asphalts was different; short-term aging significantly affected HVMA, whereas long-term aging had an enormous impact on CRMA. Modified asphalt aging is caused by the simultaneous oxidation of neat asphalt and degradation of the modifiers. The degree of degradation of the modifiers as well as the thermal-oxidative aging of neat asphalt at different aging stages may cause this effect

$$\text{CRRF} = \frac{\text{Aged rutting factor} - \text{Unaged rutting factor}}{\text{Unaged rutting factor}} \times 100 \quad (2)$$

Medium-Temperature Properties Analysis

Response Analysis of LAS

Fig. 6 shows the complex shear moduli of the neat asphalt, SBSMA, CRMA, and HVMA. The moduli of the four asphalt samples increased with frequency because the binder is a viscoelastic material and has a lag reaction to loads. In the loading process, it does not compress instantaneously or rebound immediately upon unloading. The energy that has been accumulated through loading cannot be instantly released. Therefore, a high loading frequency indicates significant energy accumulation. After aging, the asphalt binder's modulus increased because the binder hardens and the elasticity of the binder increases. In addition, the modulus of the binders after PAV was higher than that after RTFOT. This indicates that long-term aging has a more powerful impact on the properties of binders than short-term aging.

Fig. 7 shows the stress-strain responses of the LAS tests. Stress-strain curves of asphalt binder exhibit similar trends. The shear stress of the binder has a peak value, which can be defined as the point of fatigue failure (AASHTO 2016b). The coordinates of the fatigue failure point are used to obtain yield stress and strain.

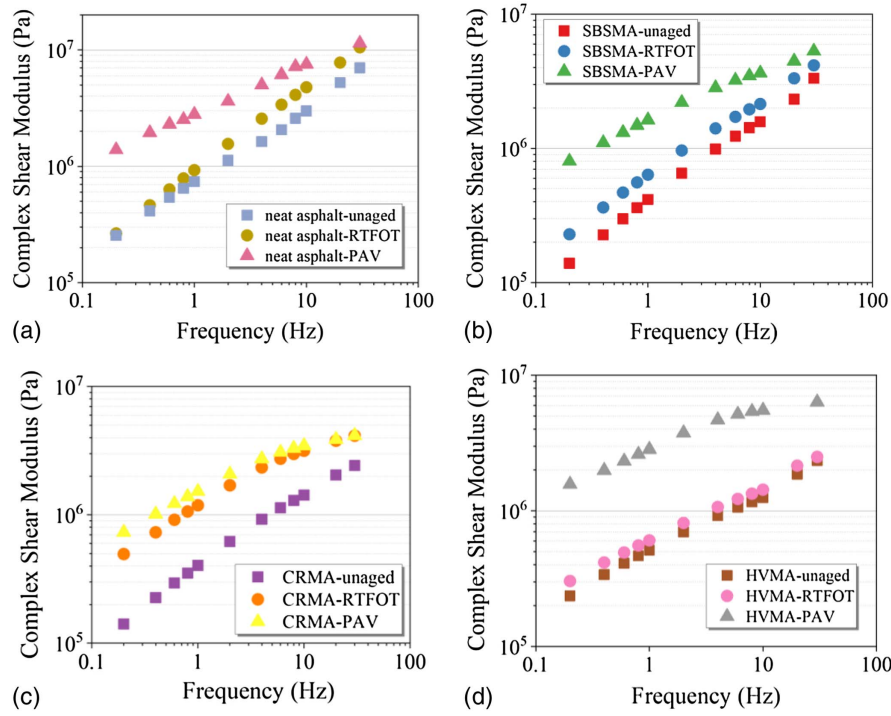


Fig. 6. Complex shear modulus from frequency sweep tests: (a) neat asphalt; (b) SBSMA; (c) CRMA; and (d) HVMA.

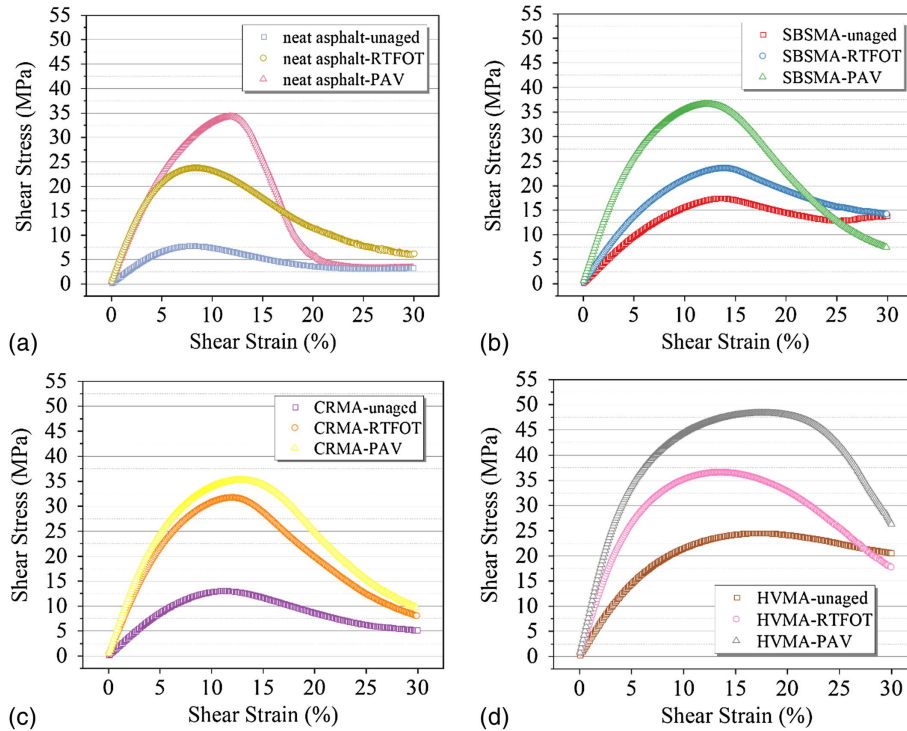


Fig. 7. Stress-strain responses of LAS tests: (a) neat asphalt; (b) SBSMA; (c) CRMA; and (d) HVMA.

After some time, the shear stress decreased sharply, indicating that the sample was damaged. As the asphalt binder aged, its yield stress increased as its aging condition deepened. However, for the yield strain, there is no apparent trend in the change after aging, suggesting that the yield stress or strain only represents the asphalt's stress-strain capacity with repeated loads. The fatigue properties of asphalt binders cannot be fully characterized by yield stress or strain.

Fatigue Life and Its Change Rate

In this study, the fatigue life of an asphalt type is computed as (AASHTO 2016b)

$$N_f = A_{35}(\gamma_{\max})^{-B} \quad (3)$$

where N_f = fatigue life; γ_{\max} = maximum expected strain of the pavement structure, which is 5.0%; and A_{35} and B are calculated as follows:

Table 2. Predicted fatigue lives of neat asphalt, SBSMA, CRMA, and HVMA

Asphalt type	Unaged			RTFOT			PAV		
	Average	Standard deviation	Grouping	Average	Standard deviation	Grouping	Average	Standard deviation	Grouping
Neat asphalt	53,009.41	201.00	D	23,292.49	239.44	D	11,627.72	474.23	D
SBSMA	524,987.58	987.08	C	282,748.38	984.12	C	227,707.29	832.95	A
CRMA	564,200.21	817.76	B	226,222.92	111.26	B	23,552.04	812.36	C
HVMA	8,714,880.00	1,707.89	A	6,430,230.00	1,071.15	A	68,284.45	1,072.90	B

1. Material constant in undamaged state α is defined as

$$\alpha = 1 + \frac{1}{m} \quad (4)$$

where m = fitting slope of the modulus master curves obtained from the frequency sweep test.

2. Parameter B is computed as

$$B = 2\alpha \quad (5)$$

where α = material constant in an undamaged state.

3. Damage variable $D(t)$ can be presented as

$$D(t) \cong \sum_{i=1}^N [\pi I_D \gamma_0^2 (|G^*| \sin \delta_{i-1} - |G^*| \sin \delta_i)]^{\alpha/(1+\alpha)} \times (t_i - t_{i-1})^{1/(1+\alpha)} \quad (6)$$

where I_D = initial modulus when the strain is equal to 1% (MPa); γ_0 = strain amplitude; G^* = modulus (MPa); δ = phase angle (degrees); α = material constant in the undamaged state; and t = test time.

4. The parameters C_0 , C_1 , and C_2 are determined as

$$|G^*| \cdot \sin \delta = C_0 - C_1(D)^{C_2} \quad (7)$$

where G^* = complex shear modulus (MPa); δ = phase angle (degrees); and D = damage variable.

5. Parameter k is evaluated as

$$k = 1 + (1 - C_2)\alpha \quad (8)$$

where C_2 = parameter calculated in Step 4; and α = material constant in the undamaged state.

6. Parameter A_{35} is determined as

$$A_{35} = \frac{f(D_f)^k}{k(\pi I_D C_1 C_2)^\alpha} \quad (9)$$

where f = frequency (Hz).

The predicted fatigue lives of neat asphalt, SBSMA, CRMA, and HVMA under different conditions as listed in Table 2. ANOVA was implemented in SPSS software to compute the fatigue lives of four asphalt samples under different conditions. A multiple-comparison procedure based on the Tukey honestly significant difference (HSD) statistical groupings was implemented on the means in ANOVA, with the confidence level of 95%. Letters are used to represent the Tukey HSD statistical groupings: A, B, C, and D indicating a statistically performance property from best to worst. It was found that the rank order of N_f in the unaged condition was HVMA > CRMA > SBSMA > neat asphalt. The neat asphalt had the shortest fatigue life under the unaged condition. After RTFOT aging, the rank order of N_f was HVMA > SBSMA > CRMA > neat asphalt. However, the rank order of N_f after PAV aging was SBSMA > HVMA > CRMA > neat asphalt. The fatigue life

sequence of SBSMA and HVMA changed after the aging of PAV, which might be related to the properties of the modified asphalt. Moreover, the fatigue resistance decreased through aging due to a reduction in fatigue life at 5.0% strain. In addition, increasing the degree of aging could decrease the fatigue life.

Accordingly, CRN_f was used as an indicator for evaluating the degree of aging of the asphalt binder at medium temperatures. A larger CRN_f indicates that aging has a greater influence on the medium-temperature fatigue properties of asphalt binders. The equation of CRN_f is

$$CRN_f = \frac{|Aged N_f - Unaged N_f|}{Unaged N_f} \times 100 \quad (10)$$

Fig. 8 displays the CRN_f of the asphalt binder after RTFOT and PAV. It can be observed that among the four asphalt samples after RTFOT, CRMA has the largest CRN_f (59.9%), indicating that aging had the most significant influence on the medium-temperature fatigue properties of CRMA. After PAV, compared with neat asphalt (78.1%), CRMA (95.8%), and SBSMA (56.6%), HVMA (99.2%) had the highest CRN_f . The fatigue property of HVMA appears to be most influenced by long-term aging at medium temperature.

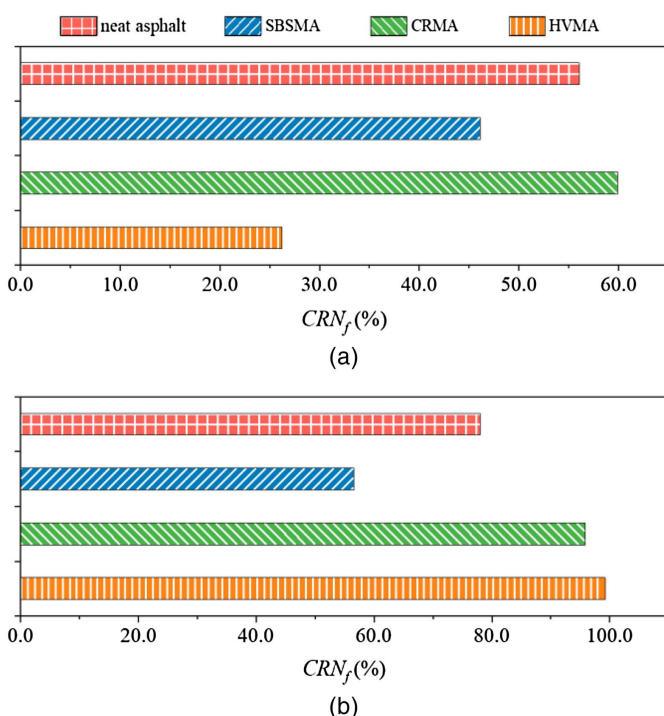


Fig. 8. Values for CRN_f of SBSMA, CRMA and HVMA: (a) RTFOT; and (b) PAV.

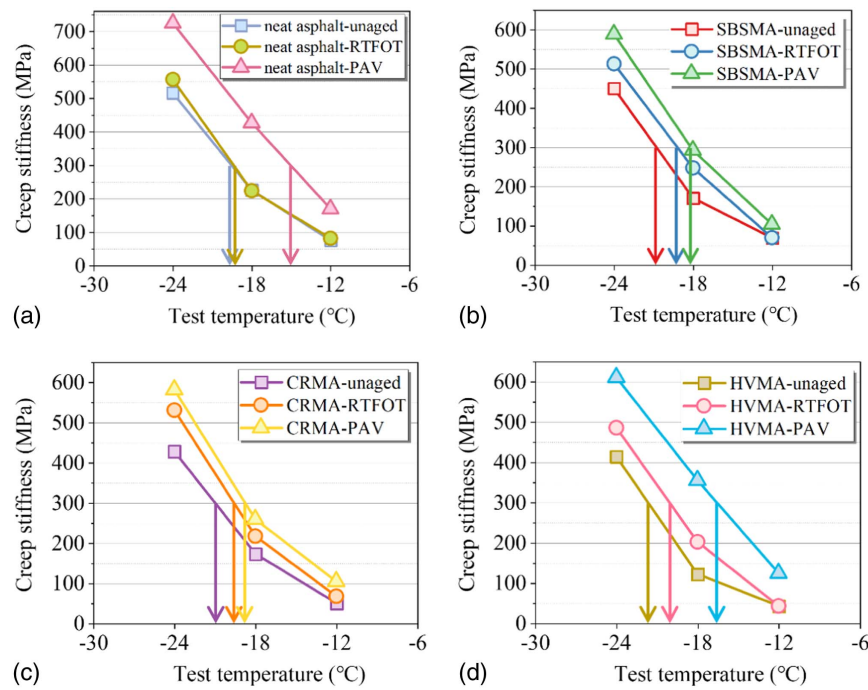


Fig. 9. Creep stiffness of modified asphalt binders versus temperature: (a) neat asphalt; (b) SBSMA; (c) CRMA; and (d) HVMA.

Low-Temperature Properties Analysis

Stiffness Value and *m*-Value

When it comes to evaluating the low-temperature cracking resistance of an asphalt binder, creep stiffness and creep rate can be used as critical indexes in the BBR test (Xiao et al. 2017). Generally, a higher creep stiffness reflects a higher tensile stress, whereas the low creep rate implies less stress relaxation (Jia et al. 2019). The creep stiffness and creep rate of the four binders in the unaged and

aged states are illustrated in Figs. 9 and 10, respectively. As a result, aged asphalt binders exhibited significantly more creep stiffness and less creep rate than unaged binders, indicating that aging decreases the low-temperature properties of the asphalt binder. After aging, the asphalt's low molecular weight components decreased, while its macromolecular components increased. This led to the modified asphalt binders becoming stiff and brittle. Furthermore, it can be seen that with increasing temperature, the creep stiffness of all binders decreased, while the creep rate increased. This indicated

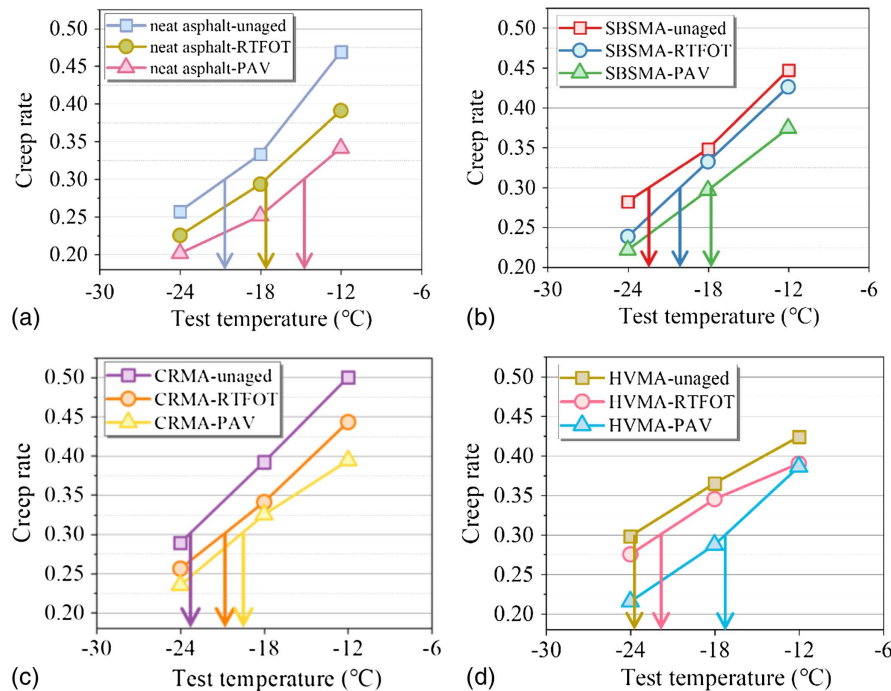


Fig. 10. Creep rate of modified asphalt binders versus temperature: (a) neat asphalt; (b) SBSMA; (c) CRMA; and (d) HVMA.

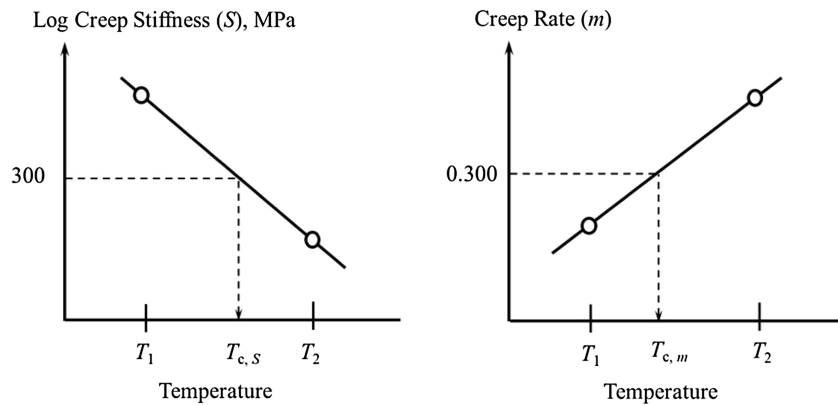


Fig. 11. Graphical concept of $T_{c,S}$ and $T_{c,m}$.

that these specimens are less inclined to crack at higher temperatures.

The low-temperature properties of the binder demand a creep stiffness smaller than 300 MPa and creep rate higher than 0.30 (Chen et al. 2019). The low-temperature properties of the modified asphalt binders reflected by creep stiffness and creep rate were consistent. Unaged binders exhibited better properties at low temperatures than RTOFT-aged binders, while RTFOT-aged binders exhibited better properties than PAV-aged binders.

Parameter ΔT_c and Its Change Rate

Parameter ΔT_c can predict the age-related embrittlement of asphalt binders at low temperature. The ΔT_c calculated from the BBR results can be used to understand the relaxation properties of asphalt binders. It is defined as the difference between $T_{c,S}$ and $T_{c,m}$ (Fig. 11) (Lesueur et al. 2021), as shown in Eq. (11). When ΔT_c is positive, the performance grade of the asphalt binder is controlled by the creep stiffness (S -controlled). When ΔT_c is negative, the performance grade of the asphalt binder is governed by the creep rate (m -controlled). Creep stiffness–governed asphalt binders fall below 300 MPa at a temperature higher than the creep rate temperature. In comparison, creep rate–governed asphalt binders exceed 0.3 creep rate at a temperature higher than the creep stiffness temperature

$$\Delta T_c = T_{c,S} - T_{c,m} \quad (11)$$

where $T_{c,S}$ = temperature at which the creep stiffness of the binder reaches 300 MPa; and $T_{c,m}$ = temperature at which the creep rate reaches 0.3; both parameters are measured in the BBR test after a loading time of 60 s.

The ΔT_c values of neat asphalt, SBSMA, CRMA, and HVMA under different aging conditions are shown in Fig. 12. This illustrates that the length of aging influences the measured values of ΔT_c . A very clear trend is that as the level of aging increases, ΔT_c reduces. This indicates that asphalt binders that cannot shed stresses become less flexible, more brittle, and more prone to cracking if subjected to applied stresses. After aging, ΔT_c for SBSMA, CRMA, and HVMA remained positive, and thus they are S -controlled. In the unaged condition, the neat asphalt indicates a positive value of ΔT_c , and hence it is S -controlled. However, RTFOT and PAV aging caused the neat asphalt to become m -controlled as indicated by the negative ΔT_c .

The $CR\Delta T_c$ can reflect the aging degree of the asphalt binder at low temperature. A higher ΔT_c indicates poor anticracking properties at low temperature. The equation of $CR\Delta T_c$ is

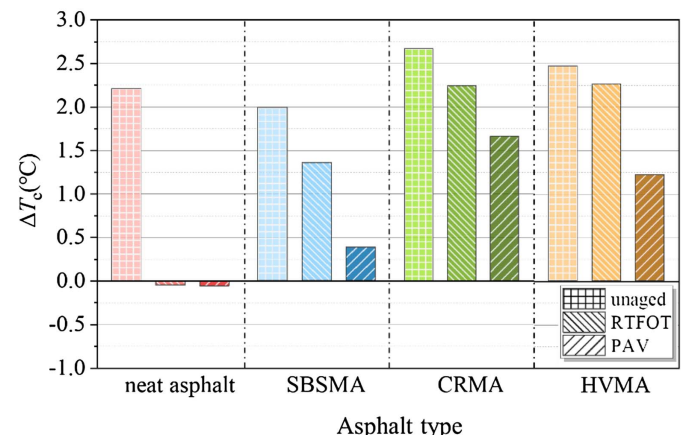


Fig. 12. Values for ΔT_c of asphalt binders under different conditions.

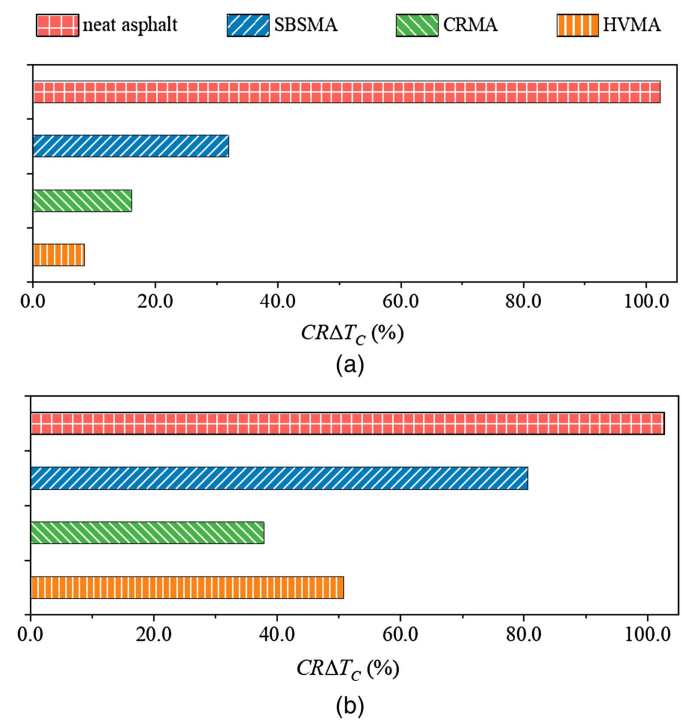


Fig. 13. $CR\Delta T_c$ of neat asphalt, SBSMA, CRMA and HVMA: (a) RTFOT; and (b) PAV.

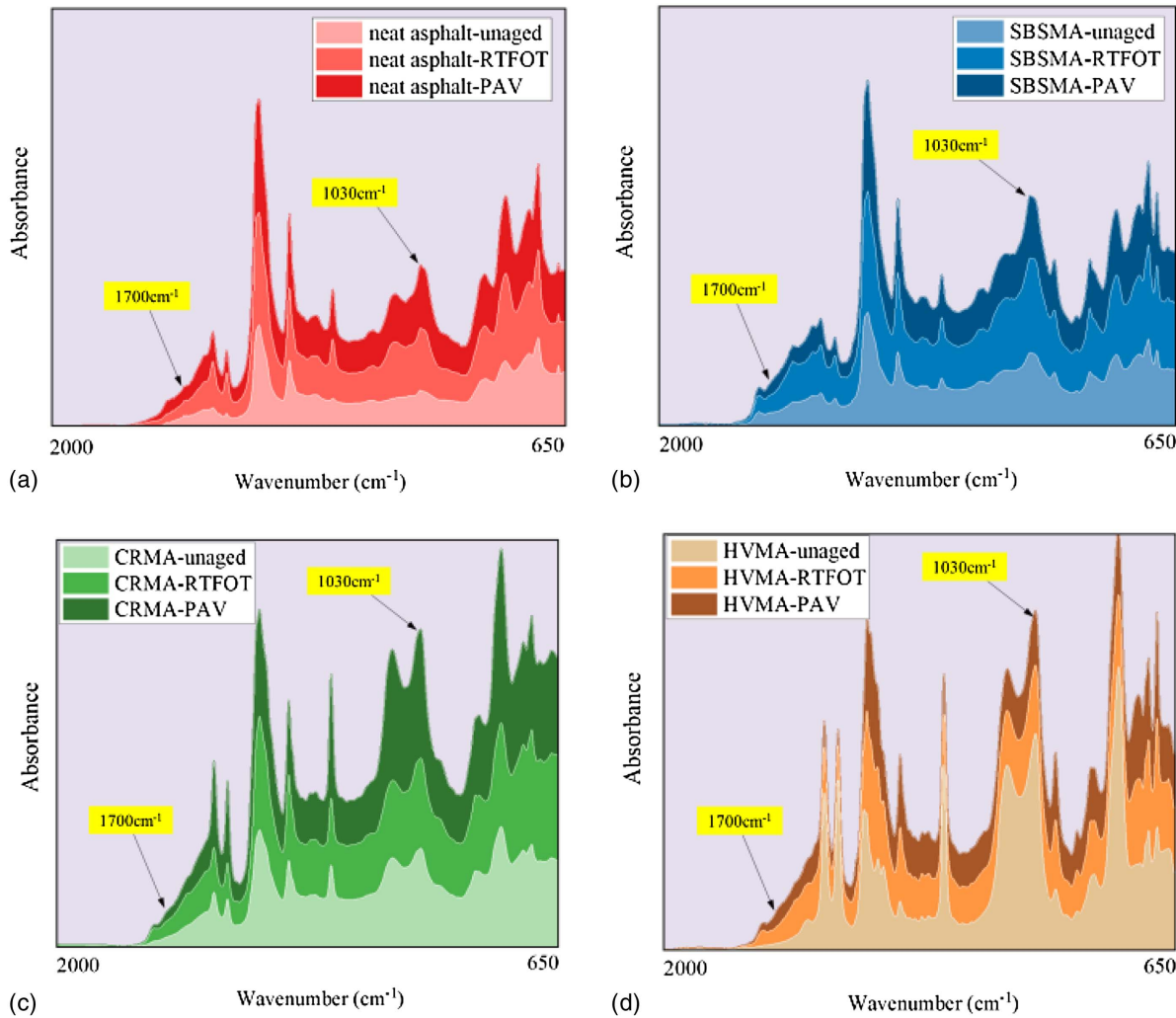


Fig. 14. FT-IR spectra of asphalt binders: (a) neat asphalt; (b) SBSMA; (c) CRMA; and (d) HVMA.

$$\text{CR}\Delta T_c = \frac{|\text{Aged } \Delta T_c - \text{Unaged } \Delta T_c|}{\text{Unaged } \Delta T_c} \times 100 \quad (12)$$

Fig. 13 shows the $\text{CR}\Delta T_c$ of neat asphalt, SBSMA, CRMA, and HVMA under different aging conditions. It can be seen that the three asphalt binders had a different $\text{CR}\Delta T_c$ after aging. A deeper degree of aging resulted in a greater $\text{CR}\Delta T_c$. For the RTFOT aging condition, the $\text{CR}\Delta T_c$ values of neat asphalt, SBSMA, CRMA, and HVMA were 102.3%, 80.6%, 16.1%, and 8.4%, respectively. For the PAV aging condition, the $\text{CR}\Delta T_c$ values of neat asphalt, SBSMA, CRMA, and HVMA were 102.8%, 80.6%, 37.8%, and 50.7%, respectively. Therefore, the $\text{CR}\Delta T_c$ ranking order of the four asphalt samples after RTFOT aging was neat asphalt > SBSMA > CRMA > HVMA. The order after PAV aging was neat asphalt > SBSMA > HVMA > CRMA. According to the results, neat asphalt had the worst low-temperature cracking resistance after aging. As for modified asphalt, compared with CRMA and HVMA, SBSMA had the worst low-temperature cracking resistance.

Microscopic Analysis

FT-IR Analysis

Fig. 14 shows the infrared spectra of the four aged samples. Here, the region in which the peaks indicate the presence of carbonyl and

sulfoxide was between 650 and 2,000 cm^{-1} . The peak areas of the carbonyl and sulfoxide functional groups were also calculated. The carbonyl index (CI) and sulfoxide index (SI) (Wang et al. 2018; Hu et al. 2018; Cavalli et al. 2018) were introduced to assess the degree of aging, as shown in Eqs. (13) and (14), respectively. First the peak intensity was normalized for calculating the CI and SI, considering the entire area under the curve to eliminate specimen thickness (Lamontagne et al. 2001)

$$\text{CI} = \frac{V(\approx 1,700)}{V(v_{\text{ref}})} \quad (13)$$

$$\text{SI} = \frac{V(\approx 1,030)}{V(v_{\text{ref}})} \quad (14)$$

where $V(v_{\text{ref}})$ = peak area at 650–2,000 cm^{-1} ; $V(\approx 1,700)$ = peak area at 1,700 cm^{-1} ; and $V(\approx 1,030)$ = peak area at 1,030 cm^{-1} . The results are presented in Fig. 14.

Fig. 15 shows that the CI of the four asphalt samples increases with aging, and the more serious the aging degree of asphalt, the larger the CI. This is due to an increase in the most polar components of the higher molecules (Zhang et al. 2011). Compared to neat asphalt, the modified asphalt had a higher CI, indicating that the three types of modified asphalt have different degrees of oxidation reaction in preparing the modified asphalt.

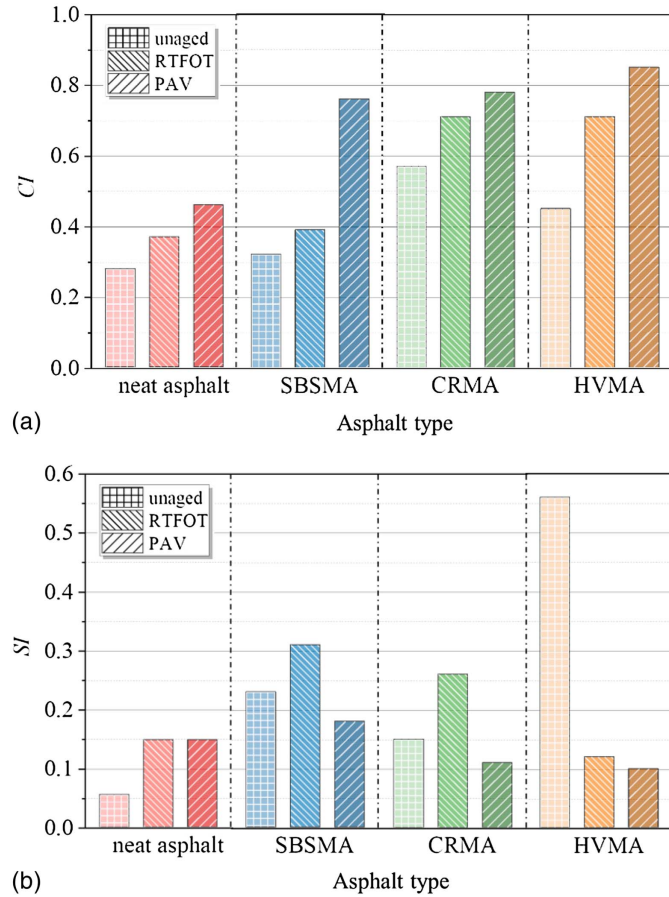


Fig. 15. (a) CI; and (b) SI of four asphalt samples under different aging conditions.

For neat asphalt, the SI increased after aging, indicating that some sulfur-oxygen double bonds ($S=O$) were formed. For SBSMA and CRMA, the SI increased after RTFOT, indicating that $S=O$ formation accompanied the oxidation reaction of SBSMA and

CRMA after short-term aging. However, the SI decreased after PAV. This is due to the moderately decomposed modifier under long-term aging, resulting in an increased sulfur content (Hou et al. 2018; Li et al. 2020b). For HVMA, the SI decreased after RTFOT, indicating that the modifier began to decompose after short-term aging. The deeper the aging degree, the greater was the decomposition of the modifier (Hu et al. 2020a).

TLC-FID Analysis

Fig. 16 shows the change of asphaltenes, resins, aromatics, and saturates of neat asphalt, SBSMA, CRMA, and HVMA in unaged, RTFOT, and PAV conditions. It can be seen that the saturates content was basically unchanged, the aromatics content decreased, and the asphaltenes and resins content increased after aging. After RTFOT, the asphaltenes content of neat asphalt, SBSMA, CRMA, and HVMA increased 19.1%, 5.4%, 2.6%, and 4.9%, respectively. Meanwhile, the resins content of neat asphalt, SBSMA, CRMA, and HVMA increased 14.3%, 13.5%, 11.9%, and 10.1%, respectively. The aromatics content of neat asphalt, SBSMA, CRMA, and HVMA decreased 9.2%, 6.8%, 9.5%, and 8.9%, respectively. Compared to modified asphalt binder, the components of neat asphalt have a higher change rate after RTFOT. For SBSMA, CRMA, and HVMA, the order change rate of components is SBSMA > HVMA > CRMA. The change of asphalt components after PAV also has the same order after RTFOT.

SEM Analysis

Fig. 17 shows the SEM images of neat asphalt, SBSMA, CRMA, and HVMA in unaged, RTFOT, and PAV conditions. The same behavior can be found in Figs. 17(a–c). With the increase of aging degree, it can be seen that the large molecular content of neat asphalt increased. Clusters were observed from Figs. 17(b and c), which may be due to the aromatization of perhydro aromatic rings (Singh and Kumar 2019). For SBSMA, CRMA, and HVMA, there are large polymer networks in unaged conditions as shown in Figs. 17(d, g, and j). After RTFOT, the polymer network begins to degrade as can be seen in Figs. 17(e and k). From Figs. 17(f, i, and l), it can be observed that the polymer network was more degraded and had an asphalt-rich phase after PAV.

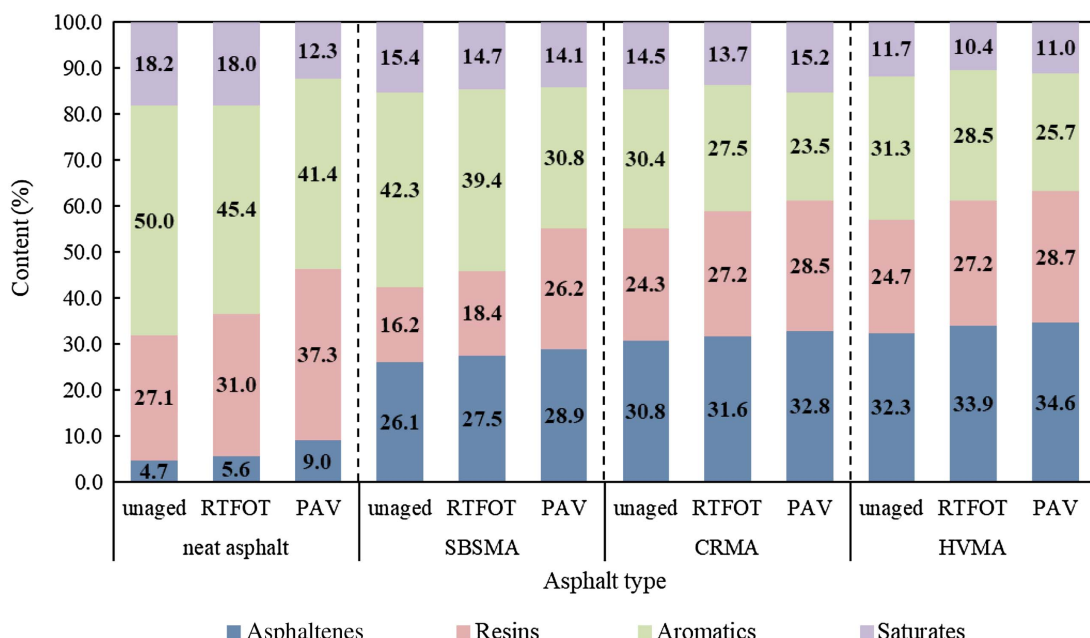


Fig. 16. Four components change of four asphalt samples under different aging conditions.

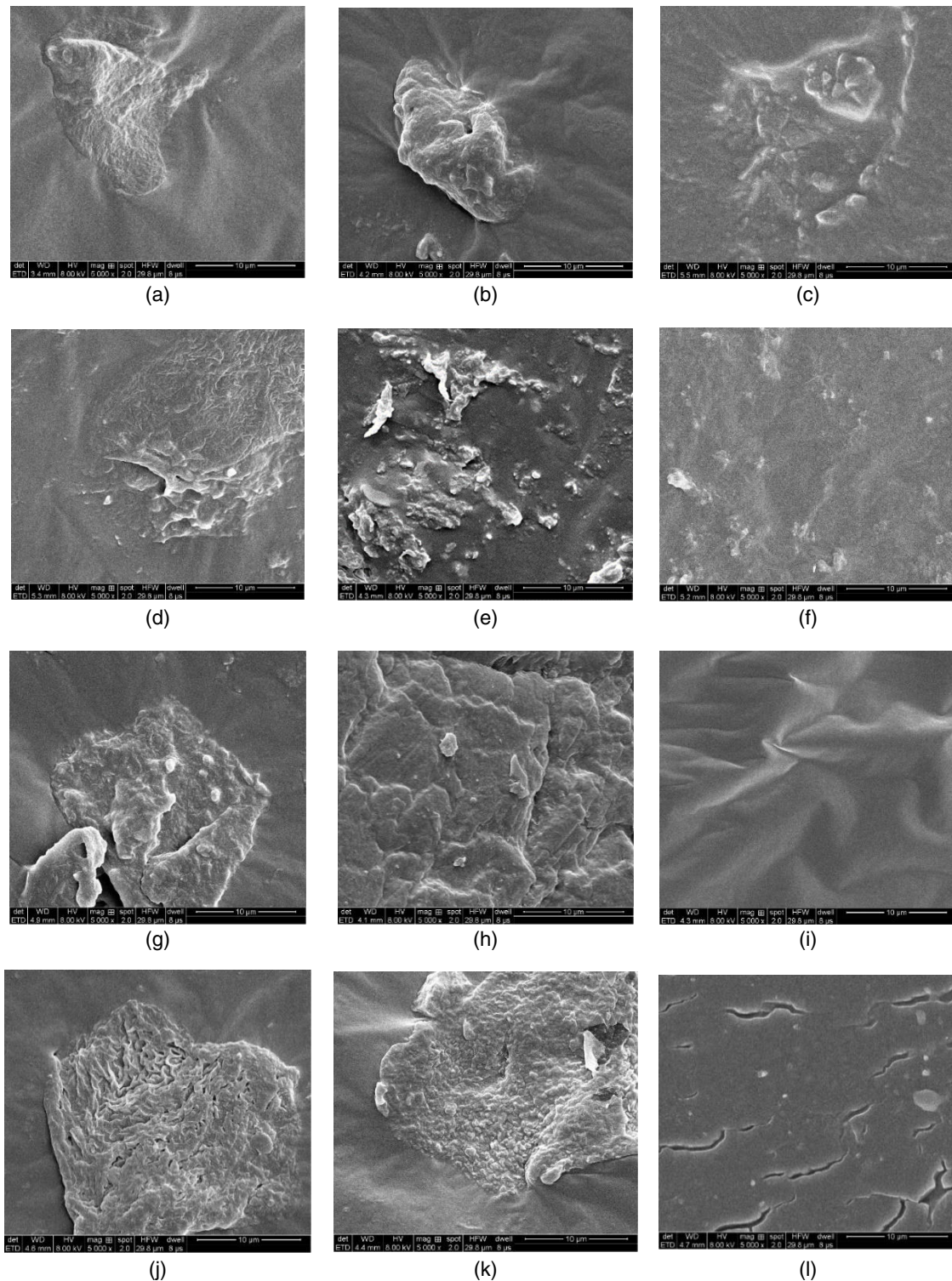


Fig. 17. SEM images of four asphalt samples under different aging conditions: (a) neat asphalt-unaged; (b) neat asphalt-RTFOT; (c) neat asphalt-PAV; (d) SBSMA-unaged; (e) SBSMA-RTFOT; (f) SMSBA-PAV; (g) CRMA-unaged; (h) CRMA-RTFOT; (i) CRMA-PAV; (j) HVMA-unaged; (k) HVMA-RTFOT; and (l) HVMA-PAV.

Conclusions

This paper assessed the aging degree quantitatively of finished product-modified asphalt binders of SBSMA, CRMA, and HVMA at high, medium, and low temperatures, and explored the aging mechanism at the microscopic level. The main conclusions are summarized as follows.

- Compared with SBSMA, CRMA, and HVMA, aging has the greatest impact on the high-, medium-, and low-temperature neat asphalt properties.
- Aging can enhance the high-temperature stability of asphalt binders. The effects of the aging degree on the high-temperature properties of the polymer-modified asphalt binders were different. After short-term aging, the CRRFs of SBSMA, CRMA, and

- HVMA were 12.6%, 7.1%, and 18.9%, respectively. After long-term aging, the CRRFs of SBSMA, CRMA, and HVMA were 159.0%, 179.5%, and 19.3%. Short-term aging significantly impacted HVMA, while long-term aging had an enormous influence on CRMA.
- Aging could decrease the fatigue resistance of an asphalt binder. Moreover, increasing the degree of aging could decrease the fatigue life. After short-term aging, the CRN_f values of SBSMA, CRMA, and HVMA were 46.1%, 59.9%, and 26.2%, respectively. After long-term aging, the CRN_f values of SBSMA, CRMA, and HVMA were 56.6%, 95.8%, and 99.2%, respectively. Short-term aging had the most significant influence on the fatigue property at medium temperature of CRMA, followed by SBSMA and HVMA. The effect of long-term aging on the fatigue properties of HVMA was the largest, followed by that of CRMA and SBSMA.
 - SBSMA, CRMA, and HVMA are *S*-controlled asphalt binders under different aging conditions. Aging caused the binders to become brittle and crack easily. After short-term aging, the $CR\Delta T_c$ values of SBSMA, CRMA, and HVMA were 80.6%, 16.1%, and 8.4%, respectively. After long-term aging, the $CR\Delta T_c$ values of SBSMA, CRMA, and HVMA were 80.6%, 37.8%, and 50.7%. Short-term aging had the most significant influence on the low-temperature properties of SBSMA, followed by CRMA and HVMA. The effect of long-term aging on the low-temperature properties of SBSMA was the largest, followed by that of HVMA and CRMA.
 - During the aging process, the oxidation reaction of asphalt was accompanied by the formation of sulfur-oxygen double bonds. After aging, the saturates content was basically unchanged, the aromatics content decreased, and the asphaltenes and resins content increased. With the increase of aging degree, it can be seen that the large molecular content of neat asphalt increased. For SBSMA, CRMA, and HVMA, the polymer network begins to degrade after aging.
 - In this study, the influence of thermal-oxidative aging on SBSMA, CRMA, and HVMA was discussed; however, the influence of ultraviolet aging on modified asphalt was not considered. In future research, the aging behavior of different modified asphalts under different aging times and coupled aging will be studied. This work studied SBSMA, CRMA, and HVMA. The follow-up study will consider comparing more types of modified asphalt.

Data Availability Statement

All data, models, and code generated or used during the study appear in the published article.

Acknowledgments

This project was jointly supported by the National Key R&D Program of China (Grant No. 2018YFB1600200), the National Natural Science Foundation of China (Grant Nos. 52122809 and 52038001), the Fok Ying-Tong Education Foundation (Grant No. 161072), the Youth Top-notch Talent Support Program of Shaanxi Province, and the Fundamental Research Funds for the Central Universities (Grant No. 300203211215).

References

- AASHTO. 2016a. *Standard method of test for determining the flexural creep stiffness of asphalt mixtures using the bending beam rheometer (BBR)*. AASHTO TP 125. Washington, DC: AASHTO.
- AASHTO. 2016b. *Standard method of test for estimating fatigue resistance of asphalt binders using the linear amplitude sweep*. AASHTO TP 101-12. Washington, DC: AASHTO.
- Airey, G. D. 2003. "Rheological properties of styrene butadiene styrene polymer modified road bitumens." *Fuel* 82 (14): 1709–1719. [https://doi.org/10.1016/S0016-2361\(03\)00146-7](https://doi.org/10.1016/S0016-2361(03)00146-7).
- Alvarez, A. E., A. E. Martin, and C. Estakhri. 2010. "Drainability of permeable friction course mixtures." *J. Mater. Civ. Eng.* 22 (6): 556–564. [https://doi.org/10.1061/\(ASCE\)MT.1943-5533.0000053](https://doi.org/10.1061/(ASCE)MT.1943-5533.0000053).
- Asgharzadeh, S. M., N. Tabatabaei, K. Naderi, and M. Parti. 2013. "An empirical model for modified bituminous binder master curves." *Mater. Struct.* 46 (9): 1459–1471. <https://doi.org/10.1617/s11527-012-9988-x>.
- ASTM. 2016. *Standard test method for determining the flexural creep stiffness of asphalt binder using the bending beam rheometer (BBR)*. ASTM D6648-08(2016). West Conshohocken, PA: ASTM.
- ASTM. 2018. *Standard test method for separation of asphalt into four fractions*. ASTM D4124-18. West Conshohocken, PA: ASTM.
- ASTM. 2019a. *Standard practice for accelerated aging of asphalt binder using a pressurized aging vessel (PAV)*. ASTM D6521-19a. West Conshohocken, PA: ASTM.
- ASTM. 2019b. *Standard test method for effect of heat and air on a moving film of asphalt (rolling thin-film oven test)*. ASTM D2872-19. West Conshohocken, PA: ASTM.
- Bi, Y., S. Wu, J. Pei, Y. Wen, and R. Li. 2020. "Correlation analysis between aging behavior and rheological indices of asphalt binder." *Constr. Build. Mater.* 264 (1): 120176. <https://doi.org/10.1016/j.conbuildmat.2020.120176>.
- Cai, J., C. Song, B. Zhou, Y. Tian, R. Li, J. Zhang, and J. Pei. 2019. "Investigation on high-viscosity asphalt binder for permeable asphalt concrete with waste materials." *J. Cleaner Prod.* 228 (Aug): 40–51. <https://doi.org/10.1016/j.jclepro.2019.04.010>.
- Cai, J., Y. Wen, D. Wang, R. Li, J. Zhang, J. Pei, and J. Xie. 2020. "Investigation on the cohesion and adhesion behavior of high-viscosity asphalt binders by bonding tensile testing apparatus." *Constr. Build. Mater.* 261 (Nov): 120011. <https://doi.org/10.1016/j.conbuildmat.2020.120011>.
- Cavallini, M. C., M. Zaumanis, E. Mazza, M. N. Partl, and L. D. Poulikakos. 2018. "Effect of ageing on the mechanical and chemical properties of binder from RAP treated with bio-based rejuvenators." *Composites, Part B* 141 (May): 174–181. <https://doi.org/10.1016/j.compositesb.2017.12.060>.
- Chen, Z., T. Wang, J. Pei, S. Amirkhanian, F. Xiao, Q. Ye, and Z. Fan. 2019. "Low temperature and fatigue characteristics of treated crumb rubber modified asphalt after a long term aging procedure." *J. Cleaner Prod.* 234 (Oct): 1262–1274. <https://doi.org/10.1016/j.jclepro.2019.06.147>.
- Cong, P., S. Chen, J. Yu, and S. Wu. 2010. "Effects of aging on the properties of modified asphalt binder with flame retardants." *Constr. Build. Mater.* 24 (12): 2554–2558. <https://doi.org/10.1016/j.conbuildmat.2010.05.022>.
- Dai, J., F. Ma, Z. Fu, C. Li, M. Jia, K. Shi, Y. Wen, and W. Wang. 2021. "Applicability assessment of stearic acid/palmitic acid binary eutectic phase change material in cooling pavement." *Renewable Energy* 175 (Sep): 748–759. <https://doi.org/10.1016/j.renene.2021.05.063>.
- Ding, X., L. Chen, T. Ma, H. Ma, L. Gu, T. Chen, and Y. Ma. 2019. "Laboratory investigation of the recycled asphalt concrete with stable crumb rubber asphalt binder." *Constr. Build. Mater.* 203 (10): 552–557. <https://doi.org/10.1016/j.conbuildmat.2019.01.114>.
- Fethiza Ali, B., K. Soudani, and S. Haddadi. 2020. "Effect of waste plastic and crumb rubber on the thermal oxidative aging of modified bitumen." *Road Mater. Pavement* 23 (1): 222–233. <https://doi.org/10.1080/14680629.2020.1820893>.
- Fini, E. H., E. W. Kalberer, A. Shahbazi, M. Basti, Z. You, H. Ozer, and Q. Aurangzeb. 2011. "Chemical characterization of biobinder from swine manure: Sustainable modifier for asphalt binder." *J. Mater. Civil Eng.* 23 (11): 1506–1513. [https://doi.org/10.1061/\(ASCE\)MT.1943-5533.0000237](https://doi.org/10.1061/(ASCE)MT.1943-5533.0000237).
- Frigio, F., E. Pasquini, M. N. Partl, and F. Canestrari. 2015. "Use of reclaimed asphalt in porous asphalt mixtures: Laboratory and field

- evaluations.” *J. Mater. Civ. Eng.* 27 (7): 04014211. [https://doi.org/10.1061/\(ASCE\)MT.1943-5533.0001182](https://doi.org/10.1061/(ASCE)MT.1943-5533.0001182).
- Gao, J., H. Wang, C. Liu, D. Ge, Z. You, and M. Yu. 2019. “High-temperature rheological behavior and fatigue performance of lignin modified asphalt binder.” *Constr. Build. Mater.* 230 (Jan): 117063. <https://doi.org/10.1016/j.conbuildmat.2019.117063>.
- Han, Z., A. Sha, L. Hu, and L. Jiao. 2021. “Modeling to simulate inverted asphalt pavement testing: An emphasis on cracks in the semirigid sub-base.” *Constr. Build. Mater.* 306 (Nov): 124790. <https://doi.org/10.1016/j.conbuildmat.2021.124790>.
- Hossain, K., A. Karakas, and Z. Hossain. 2018. “Effect of aging and rejuvenation on surface-free energy measurements and adhesive property of asphalt mixtures.” *J. Mater. Civ. Eng.* 31 (7): 04019125. [https://doi.org/10.1061/\(ASCE\)MT.1943-5533.0002780](https://doi.org/10.1061/(ASCE)MT.1943-5533.0002780).
- Hou, X., F. Xiao, J. Wang, and S. Amirkhanian. 2018. “Identification of asphalt aging characterization by spectrophotometry technique.” *Fuel* 226 (Aug): 230–239. <https://doi.org/10.1016/j.fuel.2018.04.030>.
- Hu, J., S. Wu, Q. Liu, M. I. G. Hernández, and W. Zeng. 2018. “Effect of ultraviolet radiation on bitumen by different ageing procedures.” *Constr. Build. Mater.* 163 (Feb): 73–79. <https://doi.org/10.1016/j.conbuildmat.2017.12.014>.
- Hu, M., D. Sun, Y. Zhang, F. Yu, and J. Ma. 2020a. “Evaluation of weathering aging on resistance of high viscosity modified asphalt to permanent deformation and fatigue damage.” *Constr. Build. Mater.* 264 (Dec): 120683. <https://doi.org/10.1016/j.conbuildmat.2020.120683>.
- Hu, M., G. Sun, D. Sun, T. Lu, and Y. Deng. 2020b. “Accelerated weathering simulation on rheological properties and chemical structure of high viscosity modified asphalt: A temperature acceleration effect analysis.” *Constr. Build. Mater.* 268 (4): 121120. <https://doi.org/10.1016/j.conbuildmat.2020.121120>.
- Hu, M., G. Sun, D. Sun, Y. Zhang, and T. Lu. 2020c. “Effect of thermal aging on high viscosity modified asphalt binder: Rheological property, chemical composition and phase morphology.” *Constr. Build. Mater.* 241 (Apr): 118023. <https://doi.org/10.1016/j.conbuildmat.2020.118023>.
- Israel, R. F., T. B. Farrokh, C. C. Maria, D. P. Lily, and B. Moises. 2020. “Microstructure analysis and mechanical performance of crumb rubber modified asphalt concrete using the dry process.” *Constr. Build. Mater.* 259 (Oct): 119662. <https://doi.org/10.1016/j.conbuildmat.2020.119662>.
- Jia, M., Z. Zhang, H. Liu, B. Peng, H. Zhang, W. Lv, Q. Zhang, and Z. Mao. 2019. “The synergistic effect of organic montmorillonite and thermoplastic polyurethane on properties of asphalt binder.” *Constr. Build. Mater.* 229 (Dec): 116867. <https://doi.org/10.1016/j.conbuildmat.2019.116867>.
- Jiang, W., Y. Huang, and A. Sha. 2018. “A review of eco-friendly functional road materials.” *Constr. Build. Mater.* 191 (Dec): 1082–1092. <https://doi.org/10.1016/j.conbuildmat.2018.10.082>.
- Jiang, W., D. Yuan, J. Shan, W. Ye, H. Lu, and A. Sha. 2020. “Experimental study of the performance of porous ultra-thin asphalt overlay.” *Int. J. Pavement Eng.* <https://doi.org/10.1080/10298436.2020.1837826>.
- Jiang, W., D. Yuan, Z. Tong, A. Sha, J. Xiao, M. Jia, W. Ye, and W. Wang. 2021. “Aging effects on rheological properties of high viscosity modified asphalt.” *J. Traffic Transp. Eng.* <https://kns.cnki.net/kcms/detail/61.1494.U.20210322.0959.002.html>.
- Lamontagne, J., P. Dumas, V. Mouillet, and J. Kister. 2001. “Comparison by Fourier transform infrared (FTIR) spectroscopy of different ageing techniques: Application to road bitumens.” *Fuel* 80 (4): 483–488. [https://doi.org/10.1016/S0016-2361\(00\)00121-6](https://doi.org/10.1016/S0016-2361(00)00121-6).
- Leng, Z., R. K. Padhan, and A. Sreeram. 2018. “Production of a sustainable paving material through chemical recycling of waste PET into crumb rubber modified asphalt.” *J. Cleaner Prod.* 180 (10): 682–688. <https://doi.org/10.1016/j.jclepro.2018.01.171>.
- Lesueur, D., M. Elwardany, J. P. Planche, D. Christensen, and G. N. King. 2021. “Impact of the asphalt binder rheological behavior on the value of the ΔT_c parameter.” *Constr. Build. Mater.* 293 (1–2): 123464. <https://doi.org/10.1016/j.conbuildmat.2021.123464>.
- Li, J., F. Xiao, and S. N. Amirkhanian. 2020a. “Rheological and chemical characterization of plasma-treated rubberized asphalt using customized extraction method.” *Fuel* 264 (15): 116819. <https://doi.org/10.1016/j.fuel.2019.116819>.
- Li, J., F. P. Xiao, and S. N. Amirkhanian. 2020b. “High temperature rheological characteristics of plasma-treated crumb rubber modified binders.” *Constr. Build. Mater.* 236 (Mar): 117614. <https://doi.org/10.1016/j.conbuildmat.2019.117614>.
- Liu, H., A. Sha, Z. Tong, and J. Gao. 2018. “Autonomous microscopic bunch inspection using region-based deep learning for evaluating graphite powder dispersion.” *Constr. Build. Mater.* 173 (Jun): 525–539. <https://doi.org/10.1016/j.conbuildmat.2018.04.050>.
- Lyu, L., D. Li, Y. Chen, Y. Tian, and J. Pei. 2021. “Dynamic chemistry based self-healing of asphalt modified by diselenide-crosslinked polyurethane elastomer.” *Constr. Build. Mater.* 293 (Jul): 123480. <https://doi.org/10.1016/j.conbuildmat.2021.123480>.
- Ma, T., H. Wang, L. He, Y. Zhao, X. Huang, and J. Chen. 2017. “Property characterization of asphalt binders and mixtures modified by different crumb rubbers.” *J. Mater. Civ. Eng.* 29 (7): 04017036. [https://doi.org/10.1061/\(ASCE\)MT.1943-5533.0001890](https://doi.org/10.1061/(ASCE)MT.1943-5533.0001890).
- Moriyoshi, A., T. Jin, T. Nakai, and H. Ishikawa. 2013. “Evaluation methods for porous asphalt pavement in service for fourteen years.” *Constr. Build. Mater.* 42 (May): 190–195. <https://doi.org/10.1016/j.conbuildmat.2012.12.070>.
- Naderi, K., S. M. Asgharzadeh, N. Tabatabaei, and M. N. Partl. 2014. “Evaluating aging properties of crumb rubber and styrene-butadiene-styrene modified binders using double logistic master curve model.” *Transp. Res.* 2444 (1): 110–119. <https://doi.org/10.3141/2444-13>.
- Singh, B., and P. Kumar. 2019. “Effect of polymer modification on the ageing properties of asphalt binders: Chemical and morphological investigation.” *Constr. Build. Mater.* 205 (Apr): 633–641. <https://doi.org/10.1016/j.conbuildmat.2019.02.050>.
- Sumit, K. S., P. Akanksha, and S. R. Sham. 2022. “Effect of additives on the thermal stability of SBS modified binders during storage at elevated temperatures.” *Constr. Build. Mater.* 314 (Jan): 125609. <https://doi.org/10.1016/j.conbuildmat.2021.125609>.
- Tang, N. P., Q. Lv, W. D. Huang, P. Lin, and C. Q. Yan. 2019. “Chemical and rheological evaluation of aging characteristics of terminal blend rubberized asphalt binder.” *Constr. Build. Mater.* 205 (Apr): 87–96. <https://doi.org/10.1016/j.conbuildmat.2019.02.008>.
- Wang, F., Y. Xiao, P. D. Cui, J. T. Lin, M. L. Li, and Z. W. Chen. 2020. “Correlation of asphalt performance indicators and aging Degrees: A review.” *Constr. Build. Mater.* 250 (Jul): 118824. <https://doi.org/10.1016/j.conbuildmat.2020.118824>.
- Wang, J., J. Yuan, K. W. Kim, and F. Xiao. 2018. “Chemical, thermal and rheological characteristics of composite polymerized asphalts.” *Fuel* 227 (1): 289–299. <https://doi.org/10.1016/j.fuel.2018.04.100>.
- Wei, C., H. Duan, H. Zhang, and Z. Chen. 2019. “Influence of SBS modifier on aging behaviors of SBS-modified asphalt.” *J. Mater. Civ. Eng.* 31 (9): 04019184. [https://doi.org/10.1061/\(ASCE\)MT.1943-5533.0002832](https://doi.org/10.1061/(ASCE)MT.1943-5533.0002832).
- Wu, S., P. Cong, and J. Yu. 2006. “Experimental investigation of related properties of asphalt binders containing various flame retardants.” *Fuel* 85 (9): 1298–1304. <https://doi.org/10.1016/j.fuel.2005.10.014>.
- Xiao, F., R. Li, H. Zhang, and S. Amirkhanian. 2017. “Low temperature performance characteristics of reclaimed asphalt pavement (RAP) mortars with virgin and aged soft binders.” *Appl. Sci.* 7 (3): 304. <https://doi.org/10.3390/app7030304>.
- Yan, C., W. Huang, Q. Lv, and P. Lin. 2019a. “Investigating the field short-term aging of high content polymer-modified asphalt.” *Int. J. Pavement Eng.* 22 (10): 1263–1272. <https://doi.org/10.1080/10298436.2019.1673390>.
- Yan, C., W. Huang, F. Xiao, L. Wang, and Y. Li. 2018. “Proposing a new infrared index quantifying the aging extent of SBS-modified asphalt.” *Road Mater. Pavement* 19 (6): 1406–1421. <https://doi.org/10.1080/14680629.2017.1318082>.
- Yan, C., W. Huang, F. Xiao, L. Wang, and Y. Li. 2019b. “Chemical and rheological evaluation of aging properties of high content SBS polymer modified asphalt.” *Fuel* 252 (Sep): 417–426. <https://doi.org/10.1016/j.fuel.2019.04.022>.
- Ye, W., W. Jiang, P. Li, D. Yuan, J. Shan, and J. Xiao. 2019. “Analysis of mechanism and time-temperature equivalent effects of asphalt binder in short-term aging.” *Constr. Build. Mater.* 215 (10): 823–838. <https://doi.org/10.1016/j.conbuildmat.2019.04.197>.

- Yusoff, N., F. M. Jakarni, V. H. Nguyen, M. R. Hainin, and G. D. Airey. 2013. "Modelling the rheological properties of bituminous binders using mathematical equations." *Constr. Build. Mater.* 40 (Mar): 174–188. <https://doi.org/10.1016/j.conbuildmat.2012.09.105>.
- Zhang, F., J. Yu, and J. Han. 2011. "Effects of thermal oxidative ageing on dynamic viscosity, TG/DTG, DTA and FTIR of SBS-and SBS/sulfur-modified asphalts." *Constr. Build. Mater.* 25 (1): 129–137. <https://doi.org/10.1016/j.conbuildmat.2010.06.048>.
- Zhang, H. L., Z. H. Chen, G. Q. Xu, and C. J. Shi. 2018. "Evaluation of aging behaviors of asphalt binders through different rheological indices." *Fuel* 221 (Jun): 78–88. <https://doi.org/10.1016/j.fuel.2018.02.087>.
- Zhang, Z., and M. Jia. 2019. "Evaluating the effect of organic reagents on short-term aging resistance of the organic rectorite asphalt by multi-indicators." *Road Mater. Pavement* 22 (1): 215–219. <https://doi.org/10.1080/14680629.2019.1634633>.
- Zhang, Z., A. Sha, X. Liu, B. Luan, J. Gao, W. Jiang, and F. Ma. 2020. "State-of-the-art of porous asphalt pavement: Experience and considerations of mixture design." *Constr. Build. Mater.* 262 (Nov): 119998. <https://doi.org/10.1016/j.conbuildmat.2020.119998>.
- Zhu, C. 2015. "Evaluation of thermal oxidative aging effect on the rheological performance of modified asphalt binders." M.S. thesis, Dept. of Civil and Environmental Engineering, Univ. of Nevada.